

Renormalization-group calculations of ground-state and transport properties of ultrasmall tunnel junctions

H. O. Frota* and Karsten Flensberg[†]

*Department of Physics, University of Tennessee, Knoxville, Tennessee 37996
and Solid State Division, Oak Ridge National Laboratory, Oak Ridge, Tennessee 37831*

(Received 16 April 1992)

We have done a numerical renormalization-group calculation for a Hamiltonian modeling charging effect in ultrasmall tunnel junctions. We find that the conductance is enhanced by the quantum charge fluctuations allowing tunneling below the charging energy gap. However, in all cases the conductance is found to vanish at zero frequency.

The tunneling of a single electron in a tunnel junction charges the capacitor C made up by the junction and—in a semiclassical picture—the tunneling electron must therefore have an energy $e^2/2C$ to overcome this energy barrier. This is what is called the “Coulomb blockade.”^{1,2} Recent experimental^{3–6} and theoretical^{7–18} works have made it clear that quantum charge fluctuations must be added to this picture. Charge fluctuations induced by the coupling to the electromagnetic environments are very important when the impedance of the surrounding circuit is lower than the quantum of resistance: $R_H = h/e^2$, as was shown by Devoret *et al.*¹¹ and Girvin *et al.*¹⁰ The theories of these authors are in reasonable qualitative agreement with experiments for large resistance junctions.¹⁹ However, the important question of the role of the charge fluctuations induced by multiple tunnelings through the barrier remains open. In Ref. 13 it was shown that these fluctuations may be included approximately as a renormalization of the environment impedance seen by the junction. It has been suggested that the junction may undergo a transition to a conducting state.^{14–16} However, the existence of a true transition is still an unsettled question. Zwerger and Scharpf¹⁷ argue that the conductance always vanishes at zero temperature but that deviations from Ohmic behavior will only be observed at exponentially small temperatures. Experiments indeed show that the Coulomb blockade is suppressed as the bare tunnel junction conductance is increased.^{5–7} The purpose of this paper is to examine the importance of the charge-transfer fluctuations.

We present numerical renormalization-group (RG) calculations which show that for a simple Hamiltonian, often used to model charging effect in tunnel junctions, the conductance at zero bias is always zero and that frequency-dependent conductance vanishes as a power law as the frequency approaches zero. The renormalization-group calculation is very different from the previous approaches in Refs. 7, 9 and 12–18 which were based on a second-order cumulant expansion in the tunneling term,^{2,20} which is only valid in the limit of infinitely many channels. This approximation neglects the coherence between the electron-hole pairs. In the RG calculation, where the Hamiltonian including the tunneling term is diagonalized directly, all coherence effects are maintained.

The renormalization-group calculation done here differs from the RG calculations for single impurity Hamiltonians (see, e.g., Ref. 21 and references therein) invented by Wilson²² in that the correlation term enters in all iterations as opposed to the impurity models where the correlation term enters only in the first iteration. The model Hamiltonian defined below is two coupled bands with a correlation term given by the *total* charge difference between them. We find that the appearance of the charging term in all iterations does not give problems with convergence.

The Hamiltonian that we study is

$$H = H_0 + H_T = H_U, \quad (1)$$

$$H_0 = \sum_k \epsilon_k c_k^\dagger c_k + \sum_p \epsilon_k d_k^\dagger d_k, \quad (2)$$

$$H_T = \frac{T}{\nu} \sum_{kk'} (c_k^\dagger d_{k'} + \text{H.c.}), \quad (3)$$

$$H_U = UQ^2, \quad (4)$$

where c, d are operators for electrons in the left and right electrodes, T is the tunneling matrix element, ν is the normalization volume, and the charge difference is $Q = (N_L - N_R)/2$, where $N_{L(R)} = \sum_k c_k^\dagger c_k$ ($d_k^\dagger d_k$). The energy U , usually of the order of millielectron volts, is given by the capacitance of the junction: $U = e^2/2C$. The charging energy is thus given by the total charge difference between the two sides, which means that the charge is instantaneously converted to a surface charge after a tunneling event. Since the redistribution of the charge happens on the scale of the plasma frequency this is a good approximation for the low energies. We have, furthermore, done the approximation that the tunneling matrix is *constant* up to a cutoff energy, D , which we take to be the half bandwidth.

The transformation of the conductance bands to the Wilson basis follows that of Wilson²² and Frota and Olivera²³ where the method of Wilson was extended to calculations of dynamical properties. The bands are discretized in logarithmic intervals: $\epsilon_0, \epsilon_n = \Lambda^{-n-z} D$, where n is an integer, $\Lambda > 1$ and z , as we will explain later, can be varied continuously. By a canonical transformation the Hamiltonian is converted to a tridiagonal basis.

The advantage of the transformation is that the two bands coupled only through the first ‘‘orbital’’ in the new basis. The Hamiltonian can then be solved iteratively, where each iteration, because of the logarithmic discretization, gives a new energy scale. For the Hamiltonian for the N th iteration we obtain²⁴

$$H_N = \Lambda^{(N-1)/2} \left[\sum_{n=0}^{N-1} \xi_n(z) (f_n^\dagger f_{n+1} + g_n^\dagger g_{n+1} + \text{H.c.}) + \tilde{T} (f_0^\dagger g_0 + \text{H.c.}) + \tilde{U} Q_N^2 \right], \quad (5)$$

where

$$Q_N = \sum_{n=0}^N (f_n^\dagger f_n - g_n^\dagger g_n), \quad (6)$$

$$f_0(g_0) = \frac{1}{\sqrt{2\nu}} \sum_k c_k(d_k), \quad (7)$$

and where $\tilde{T} = 4T / [(1 + \Lambda^{-1})D]$, $\tilde{U} = U / [2(1 + \Lambda^{-1})D]$. The Hamiltonian (5) has been multiplied by the factor $2\Lambda^{(N-1)/2} / [(1 + \Lambda^{-1})D]$ so that H_N is of order 1. The transformation between the energies ϵ_k in the original Hamiltonian equation (1) and the hopping elements $\xi_n(z)$ in the tridiagonal basis is a function of z and, in contrast to the Wilson discretization, must be found numerically by a recursive method.^{21,23} For large n they are given by $\xi_n \sim \Lambda^{1-z-n/2}$. It is important to note that ξ_n do not depend on the parameters of the Hamiltonian other than the bandwidth D , which sets the energy scale. The energies ξ_n simply define the correspondence between the diagonal basis of H_0 and the tridiagonal basis used in Eq. (5).

From Eq. (5), we can express the Hamiltonian for the $N+1$ step in terms of H_N and Q_N and obtain the recursion formula

$$H_{N+1} = \Lambda^{1/2} H_N + \Lambda^{N/2} h_N + 2\Lambda^{N/2} \tilde{U} Q_N q_{N+1} + \Lambda^{N/2} \tilde{U} q_{N+1}^2, \quad (8)$$

$$h_N = \xi_n \left[f_N^\dagger f_{N+1} + g_N^\dagger g_{N+1} + \text{H.c.} \right], \quad (9)$$

$$q_N = f_N^\dagger f_N - g_N^\dagger g_N. \quad (10)$$

From one iteration to the next the basis set is enlarged by the states, $f_{N+1}^\dagger |\Psi_N\rangle$, $g_{N+1}^\dagger |\Psi_N\rangle$, and $f_{N+1}^\dagger g_{N+1}^\dagger |\Psi_N\rangle$, where $|\Psi_N\rangle$ is a state in a basis set for H_N . The matrix is diagonalized in the basis spanned by the eigenstates of H_N . In each iteration we also keep the matrix element of Q_N , and I_N , where I is the current operator defined below. After the diagonalization we keep only the lowest-energy states, typically 450 states. The iterative process is continued to N of the order 20, where the eigenvalues are converged within less than 2%. We turn next to the results of the RG calculation of the ground-state and transport properties.

Ground-state properties. We have calculated the average charge transfer in the ground state, i.e., the expectation value

$$\left\langle \frac{1}{\nu} \sum_{kp} c_k^\dagger d_p \right\rangle = 2 \langle f_0^\dagger g_0 \rangle = \langle H_T \rangle / 2T. \quad (11)$$

The results are shown in Fig. 1 for two different values of T . In the figure we compare with the expression for a second-order perturbation theory in the tunneling matrix element:

$$\left\langle \frac{1}{\nu} \sum_{kpt} c_k^\dagger d_p \right\rangle = -\frac{2T}{\nu} \sum_{kp} \frac{\Theta(-\epsilon_k) \Theta(\epsilon_p)}{\epsilon_p - \epsilon_k + U}. \quad (12)$$

The agreement is seen to be good for the sample with small T , as expected. We have found the *exact* $U=0$ result (derived in Appendix A) which is shown as arrows at the vertical axes. The agreement with numerical results illustrates the accuracy of the RG calculation.

The expectation value given in (11) decreases logarithmically as $\ln(U/D)$ for large U where D is the half bandwidth (we take for simplicity a half-filled band). We thus see that the correlation term effects the ground-state properties very little because of the large phase space available for virtual tunneling events. The opposite is the case for the transport properties which we study next.

Transport properties. The experimentally interesting quantity is the conductance. We calculate the frequency-dependent conductance which is given by the Kubo formula:

$$G(\omega) = \frac{\pi}{\omega} \sum_n |\langle n | I | 0 \rangle|^2 \delta(E_n - E_0 - \omega), \quad (13)$$

where $|n\rangle$ are eigenstates of the Hamiltonian and I is the current operator given by $I = ie[H, Q] = ieT \sum_{kp} (c_k^\dagger d_p - \text{H.c.})$.

In order to calculate a continuous conductance spectrum, we need a continuum of excited states. In the numerical solution we have only discrete lines and we employ the method of Frota and Olivera²³ (see also Ref. 21), where this problem was bypassed by the introduction of the extra parameter z , which shifts the discrete lines continuously. Averaging over z gives the conductance as a function of frequency:

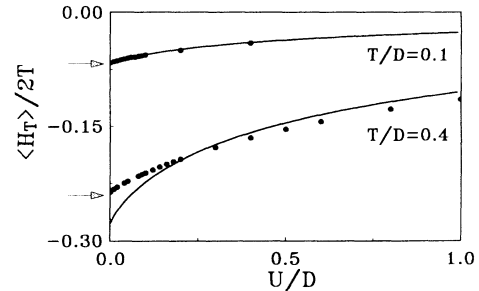


FIG. 1. The average charge transfer [see Eq. (11)] in the ground state plotted as a function of the charging energy for two values of the tunneling matrix element. The circles are the renormalization-group results and the lines are the second-order perturbation theory in T . We see that the perturbation theory describes well the ground-state properties. The arrows at the ordinate axis are the exact $U=0$ results and the agreement with the numerical calculations is excellent.

$$G(\omega) = \sum_{in(z)} \frac{|\langle n(z)|I|0\rangle|^2}{|df_n(z)/dz|_{z=z_i}}, \quad (14)$$

where z_i are the roots of the function, $f_n(z) = E_n(z) - E_0 - \omega$. This function is found numerically by running for typically 20 different values of z .

In Fig. 2 we show the results for the frequency-dependent conductance for different coupling strengths. The curves have been normalized to the *exact* large- ω (or $U=0$) asymptote. The RG calculation is thus found to give an accurate result for the conductance in the asymptotic limit. In this limit, the limiting conductance can be found exactly which is done in Appendix B, and the result is

$$G_0 = G_H \frac{4\alpha}{(1+\alpha)^2}, \quad \alpha = \pi^2 \rho^2 T^2, \quad (15)$$

where we again take a constant density of states and where the quantum of conductance is $G_H = e^2/h$. It is seen that this conductance-formula has a maximum value $G_0^{\max} = G_H$ which is reached for $\alpha=1$. We emphasize that the present model with a *constant* tunneling matrix element limits the range of conductance that we can study. The constant T is equivalent to a junction with only one connecting channel between the two sides. The

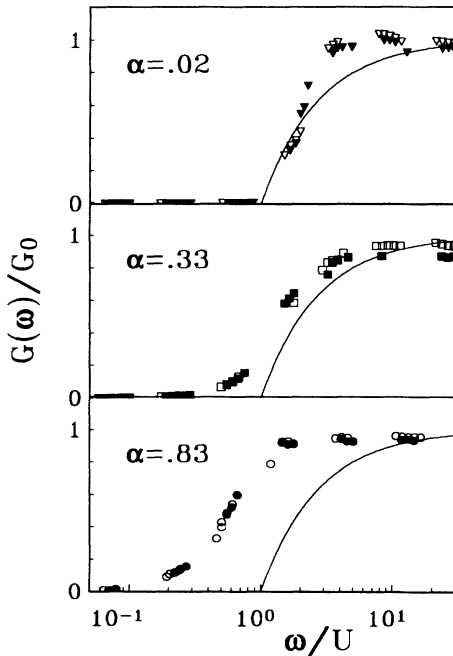


FIG. 2. The frequency-dependent conductance calculated for different values of $\alpha = \pi^2 \rho^2 T^2$, normalized to the exact result for the large- ω limit, see Eq. (15). For each α , we have shown the results for two different values of the charging energy, $U=0.001D$ (solid symbols) and $U=0.01D$ (open symbols) and the results scale with U . The lines indicate the semiclassical result in Eq. (16) (normalized to G_0^2), which is seen to be a good approximation for the data for the small α , but for larger α quantum fluctuations are important and we have a nonzero conductance for $\omega < U$ as well.

single-channel limitation is not present in the second-order cumulant expansion employed in Refs. 7, 9, and 12–16. Realistic junctions can have more channels [and the conductance formula in Eq. (15) should be replaced by the corresponding multi-channel formula] and consequently have a larger maximum conductance than G_H .

In Fig. 2, we show the results for the conductance calculated for three different values of the parameter α and for each α we have calculated for two different values of the charging energy. We see that the results do not change with U when scaled accordingly. Therefore, the model (when U is well below the band edge, which is indeed the case experimentally where U are of the order of millielectron volts) has essentially only one parameter which is the tunneling matrix element.

For small α the junction is practically “blocked” for energies below the charging energy. To second order in the tunneling matrix we get the result for this “semiclassical” limit:

$$G^{(2)} = G_H 4\alpha(1 - U/\omega)\Theta(\omega - U). \quad (16)$$

For larger values of the coupling parameter the conductance is finite for energies below the charging energy gap. This is due to quantum fluctuations or multiple tunneling events which introduce an uncertainty of the charge on the junction capacitor. The conductance therefore scales like T^4 (α^2), which is roughly the case for the curves in Fig. 3. This smearing of the Coulomb gap structure for large and intermediate values of α is clearly seen in Fig. 2. However, we find for all parameters which we have used that the conductance vanishes for zero frequency. For small energies the conductance vanishes as a power law. In Fig. 3 we show the low-frequency part of the curves in a log-log plot. The power is found to be nearly independent of α and given by ≈ 2 . This power-law dependence agrees with the perturbation expansion by Ueda and Guinea¹⁸ [In contrast, a perturbation calculation by Nazarov,¹² yields a $G(\omega) \sim \alpha^2(\omega/U)^6$ dependence.] and with the results found by Zwerger and

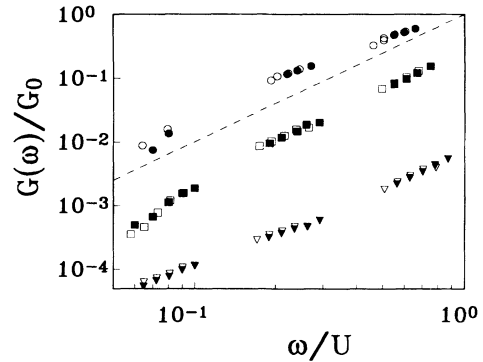


FIG. 3. The same data as in Fig. 2 plotted in log-log plot. The low-frequency part of the conductance is given by a power law where the power is approximately given by 2 and approximately independent of the nominal resistance of the junction. For clarity we have inserted a dashed line with slope 2.

Scharpf who show that the conductance vanishes as the temperature squared.

In recent Monte Carlo calculations¹⁵ it was found that as the conductance is increased there is crossover to a state which deviates from the low conductance situations where there is an algebraical decay of the correlations between backward and forward tunnelings. The crossover was claimed to indicate a transition from a blocked to a conducting phase. As explained above, we cannot make conclusions from the RG calculations about junctions with $G_0 > G_H$. However, the scaling behavior of the model leads to general conclusions, which we discuss next.

We have used a scheme closely related to the one used by Anderson²⁵ for the Kondo problem and by Haldane²⁶ for the Anderson model. The strategy is to gradually lower the high-energy cutoff by successive cutting off of a strip of the high-energy cutoff. We find from this analysis that the only nontrivial scaling is an increase of U which is continued until U is of the same order as the cutoff energy. We obtain the scaling equation for U :

$$\frac{dU}{d \ln(D)} = -\rho T^2. \quad (17)$$

The tunneling matrix element is unchanged under the scaling and hence also the current operator. We thus have only one fix point which is large U . These arguments are valid also for the general case, i.e., for junctions with more channels, which suggest that the zero conductance at $\omega=0$ found in the numerical calculation is a general feature as well. The large- U fix point is confirmed by our numerical renormalization-group calculations where we find that after approximately 20 iterations we are in a fix point where states with nonzero charge difference are projected out.

In summary, we have solved a simplified model Hamiltonian describing single-electron charging effects in small tunnel junctions. The model was solved by the numerical renormalization-group method of Wilson, and we found both the ground-state and the transport properties. While the correlation term was found to have very effect on the ground-state properties, the situation is the opposite for the conductance which in the present model is always zero at zero frequency and decreases approximately quadratically with frequency.

The authors acknowledge stimulating discussions with G. D. Mahan. The research was supported by the U.S. Department of Energy through Contact No. DE-AC05-84OR21400 administered by Martin Marietta Energy Systems, Inc., and by the University of Tennessee.

APPENDIX A

In order to find an expression for the expectation value of the tunneling term, we define the following Matsubara Green's functions:

$$G_{12}(k, k'; \tau) = \langle \mathcal{T}_\tau c_k^\dagger(\tau) d_{k'}(0) \rangle, \quad (A1)$$

$$G_{22}(k, k'; \tau) = \langle \mathcal{T}_\tau d_k^\dagger(\tau) d_{k'}(0) \rangle. \quad (A2)$$

The equations of motion are easily found and after Fourier transformation we have

$$(i\omega_n - \epsilon_k) G_{12}(k, k'; i\omega_n) = \frac{T}{\nu} \sum_{k''} G_{22}(k'', k'; i\omega_n), \quad (A3)$$

$$(i\omega_n - \epsilon_k) G_{22}(k, k'; i\omega_n) = \delta_{kk'} + \frac{T}{\nu} \sum_{k''} G_{12}(k'', k'; i\omega_n). \quad (A4)$$

If we define the functions

$$F_{ij}(k'; i\omega_n) = \sum_k G_{ij}(k, k'; i\omega_n), \quad (A5)$$

we get two coupled equations for F_{12} and F_{22} . Solving these and inserting the result back into Eqs. (A3) and (A4) leads after some algebra to the following result for the k -summed Green's functions:

$$\begin{aligned} G_{12}(i\omega_n) &\equiv \frac{1}{\nu} \sum_{kk'} G_{12}(k, k'; i\omega_n) \\ &= \frac{TF_0(i\omega_n)^2}{1 - T^2 F_0(i\omega_n)^2}, \end{aligned} \quad (A6)$$

$$\begin{aligned} G_{22}(i\omega_n) &\equiv \frac{1}{\nu} \sum_{kk'} G_{22}(k, k'; i\omega_n) \\ &= \frac{F_0(i\omega_n)}{1 - T^2 F_0(i\omega_n)^2}, \end{aligned} \quad (A7)$$

$$F_0(i\omega_n) = \frac{1}{\nu} \sum_k \frac{1}{i\omega_n - \epsilon_k}. \quad (A8)$$

From this we finally get

$$\begin{aligned} \left\langle \frac{1}{\nu} \sum_{kp} c_k^\dagger d_p \right\rangle &= \frac{1}{\nu} \sum_{k, k'} G_{12}(k, k'; \tau=0) \\ &= \frac{1}{\beta} \sum_{i\omega_n} \frac{TF_0(i\omega_n)^2}{1 - T^2 F_0(i\omega_n)^2}. \end{aligned} \quad (A9)$$

The Matsubara sum is converted to a contour integration. We can show that the Green's function only has poles on the real axes, which allows us to write the above sum as

$$\int_{-\infty}^{\infty} \frac{d\epsilon}{\pi} n_F(\epsilon) \text{Im} G_{12}(\epsilon + i\delta). \quad (A10)$$

When evaluating F_0 , we use as in the RG calculations a constant density of states and, furthermore, that the Fermi level lies in the middle of the band. We then obtain

$$F_0(\epsilon + i\delta) = \rho \ln \left| \frac{\epsilon - D}{\epsilon + D} \right| - i\pi\rho\theta(D - |\epsilon|), \quad (A11)$$

where $2D$ is the bandwidth and $\rho = 1/2D$. When doing the integral in Eq. (A10), we must include the contribution from a bound state below the band-edge. The energy of this state is given by $-D \coth(D/T)$ (and there is also one at the symmetrical position above the band). The corresponding delta-function contribution to the integral (A10) is

$$\left[\frac{D}{T \sinh(D/T)} \right]^2. \quad (\text{A12})$$

When $T \gg D$ all the spectral weight is given by (A12) whereas for small T the contribution goes to zero like $\exp(-2D/T)$. The bound state corresponds to a localized state at the junction interface in a bonding configuration (the symmetrical state above the band is the corresponding antibonding state). As is discussed in the main part and shown in Appendix B, the limit of large ρT is unphysical and the conductance has a maximum for a finite T corresponding to a completely transparent interface.

APPENDIX B

Here we calculate the conductance of the junction in the $U=0$ limit. We start with an imaginary-time current-current correlation function

$$P(\tau) = \langle \mathcal{T}_\tau I(\tau) I(0) \rangle \\ = 2e^2 [G_{22}(\tau)G_{22}(-\tau) - G_{12}(\tau)G_{12}(-\tau)]. \quad (\text{B1})$$

The Fourier-transformed correlation function becomes

$$P(i\omega_n) = \frac{1}{\beta} \sum_p G_{22}(i\omega_p) G_{22}(i\omega_p + i\omega_n) \\ \times [1 - T^2 F_0(i\omega_n) F_0(i\omega_p + i\omega_n)]. \quad (\text{B2})$$

Since we want the conductance for $\omega \ll D$, we can evaluate F at small frequencies and obtain $F(i\omega_n)^2 = \pi^2 \rho^2$. The denominators in G_{22} are thus simply constants. From this we get that the second term in Eq. (B2) is constant and real, and therefore gives no contribution to the conductance since we must take the imaginary part after analytic continuation. We can now easily calculate the conductance by performing the standard Matsubara summation and we obtain

$$G = \frac{1}{\omega} \text{Im} P(\omega + i\delta) = \frac{e^2 \pi \rho^2 T^2}{(1 + \pi^2 \rho^2 T^2)^2}, \quad (\text{B3})$$

which is Eq. (15) (note that we have used $\hbar=1$).

*Permanent address: Departamento de Física, Instituto de Ciências Exatas, Universidade do Amazonas, Manaus-Am, 69068 Brazil.

†Present address: NORDITA, Blegdamsvej 17, DK-2100 Copenhagen Ø, Denmark.

¹For a review, see D. V. Averin and K. K. Likharev, in *Mesoscopic Phenomena in Solids*, edited by B. L. Althuler, P. A. Lee, and R. A. Webb (Elsevier, Amsterdam, 1990).

²For a review, see G. Schön and A. D. Zaikin, *Phys. Rep.* **198**, 238 (1990).

³P. Delsing, K. K. Likharev, L. S. Kuzmin, and T. Claeson, *Phys. Rev. Lett.* **63**, 1180 (1989).

⁴L. J. Geerligs, V. F. Anderegg, and C. A. van der Jeugd, *Europhys. Lett.* **10**, 79 (1989).

⁵A. N. Cleland, J. M. Schmidt, and J. Clarke, *Phys. Rev. Lett.* **64**, 1565 (1990).

⁶S. Gregory (unpublished).

⁷S. V. Panyukov and A. D. Zaikin, *J. Low Temp. Phys.* **73**, 1 (1988).

⁸A. A. Odintsov, *Zh. Eksp. Teor. Fiz.* **94**, 312 (1988) [*Sov. Phys. JETP* **67**, 1265 (1988)].

⁹Yu. V. Nazarov, *Zh. Eksp. Teor. Fiz.* **95**, 975 (1989) [*Sov. Phys. JETP* **68**, 561 (1989)]; *Pis'ma Zh. Eksp. Teor. Fiz.* **49**, 1349 (1989) [*JETP Lett.* **49**, 126 (1989)].

¹⁰S. M. Girvin, L. I. Glazman, M. Jonson, D. R. Penn, and M.

D. Stiles, *Phys. Rev. Lett.* **64**, 3183 (1990).

¹¹M. H. Devoret, D. Esteve, H. Grabert, G.-L. Ingold, H. Pothier, and C. Urbina, *Phys. Rev. Lett.* **64**, 1824 (1990).

¹²Yu. V. Nazarov, *Fiz. Niz. Temp.* **16**, 718 (1990) [*Sov. J. Low Temp. Phys.* **16**, 422 (1990)].

¹³K. Flensberg and M. Jonson, *Phys. Rev. B* **43**, 7586 (1991).

¹⁴R. Brown and E. Šimánek, *Phys. Rev. B* **34**, 2957 (1986).

¹⁵V. Scalia, G. Falsi, R. Fazio, and G. Giaquinta, *Phys. Rev. Lett.* **67**, 2203 (1991).

¹⁶S. V. Panyukov and A. D. Zaikin, *Phys. Rev. Lett.* **67**, 3168 (1991).

¹⁷W. Zwerger and M. Scharpf, *Z. Phys. B* **85**, 421 (1991).

¹⁸M. Ueda and F. Guinea, *Z. Phys. B* **85**, 413 (1991).

¹⁹K. Flensberg, S. M. Girvin, M. Jonson, D. R. Penn, and M. D. Stiles, *Z. Phys. B* **85**, 395 (1991).

²⁰V. Ambegaokar, U. Eckern, and G. Schön, *Phys. Rev. Lett.* **48**, 1745 (1982).

²¹L. N. Oliveira, V. L. Libero, H. O. Frota, and M. Yoshida, *Physica B* **171**, 61 (1991).

²²K. G. Wilson, *Rev. Mod. Phys.* **47**, 773 (1975).

²³H. O. Frota and L. N. Olivera, *Phys. Rev. B* **33**, 7871 (1986).

²⁴K. Flensberg and H. O. Frota, *Solid State Commun.* **77**, (1991).

²⁵P. W. Anderson, *J. Phys. C* **3**, 2436 (1970).

²⁶F. D. M. Haldane, *Phys. Rev. Lett.* **40**, 911 (1978).